© 2001 The Chemical Society of Japan

Further Investigation on Preparation, Structure and Electrochemical Properties of *N*-Alkyl- and *N*-Aryl-2-aza-[3]-ferrocenophanes

Tatsuaki Sakano, Masaki Horie, Kohtaro Osakada,* and Hidenobu Nakao†

Chemical Resources Laboratory, Tokyo Institute of Technology, 4259 Nagatsuta, Midori-ku, Yokohama 226-8503

†Instrumentation Engineering Laboratory, National Food Research Institute, 2-1-12, Kannondai, Tsukuba 305-8642

(Received March 29, 2001)

The reactions of 1,1′-bis(hydroxymethyl)ferrocene with primary amines such as 6-aminohexanol, cyclohexylamine, 4-phenylbutylamine, 2-isopropylaniline, 4-(trifluoromethyl)benzylamine, and 1-aminomethylferrocene in the presence of $[RuCl_2(PPh_3)_3]$ catalyst led to intermolecular condensation of the CH_2OH and NH_2 groups to afford *N*-alkyl- or *N*-aryl substituted 2-aza-[3]-(1,1′)-ferrocenophanes. Cyclic voltammograms of the obtained *N*-alkyl-2-aza-[3]-(1,1′)-ferrocenophanes exhibit reversible redox of the Fe center at $E_{1/2} = -0.01 - +0.04$ V (vs Ag^+/Ag) and subsequent irreversible oxidation of the amino group of the ligand at $E_{ox} = 0.41$–0.44 V. *N*-(4-Hydroxyphenyl)-2-aza-[3]-(1,1′)-ferrocenophane shows two pairs of reversible electrochemical oxidation and reduction at $E_{1/2} = 0.04$ and 0.44 V. The latter potential is significantly lower than the corresponding electrochemical oxidation of *N*-aryl-2-aza-[3]-(1,1′)-ferrocenophanes (0.68–0.75 V). The *N*-alkyl-2-aza-[3]-(1,1′)-ferrocenophanes react with MeI to cause methylation of the amino group to produce cationic 2-aza-[3]-(1,1′)-ferrocenophanes containing a quaternary nitrogen center. The iodo counter anion is easily replaced with BF_4^- or PF_6^-. Cyclic voltammograms of the cationic ferrocenophanes show the redox between ferrocene and ferrocenium at $E_{1/2} = 0.37$–0.42 V.

Introduction of functional groups to cyclopentadienyl ligands of ferrocene provides a variety of compounds which show unique electrochemical and physical properties as potential molecular materials.[1–6] We reported previously Ru complex-catalyzed condensation of 1,1′-bis(hydroxymethyl)ferrocene with arylamines and hexylamine[7–11] to produce *N*-aryl (or alkyl)-2-aza-[3]-(1,1′)-ferrocenophanes in moderate to high yields as shown in Scheme 1.[12] In order to obtain further scope and insight of the reaction and the products, we have continued study of the condensation of 1,1′-bis(hydroxymethyl)ferrocene with various alkylamines and the chemical and electrochemical properties of the formed ferrocenophanes. Here we report preparation of several new *N*-alkyl-2-aza-[3]-(1,1′)-ferrocenophanes and related compounds, as well as results of reinvestigation of their structures and electrochemical behavior, and compare the results with those for analogous *N*-aryl-2-aza-[3]-(1,1′)-ferrocenophanes reported previously.

Results and Discussion

Alkylamines such as 6-aminohexanol, cyclohexylamine, and 4-phenylbutylamine react with 1,1′-bis(hydroxymethyl)ferrocene in the presence of $[RuCl_2(PPh_3)_3]$ catalyst at 180 °C to produce the corresponding *N*-alkyl-2-aza-[3]-(1,1′)-ferrocenophanes **1**–**3** as shown in Eq. 1.

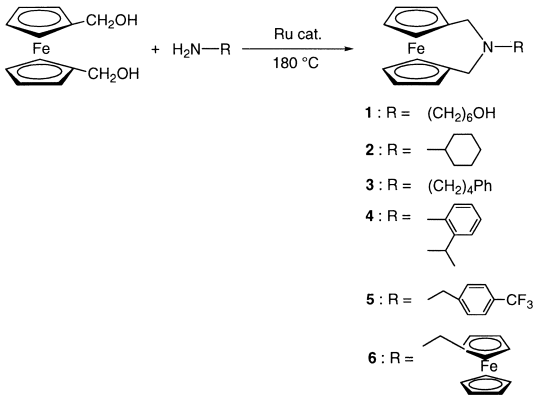

(1)

Similar reactions of 2-isopropylaniline and of 4-(trifluoromethyl)benzylamine also form the *N*-substituted-2-aza-[3]-(1,1′)-ferrocenophanes **4** and **5**, respectively. Ferrocenophane **6**, having ferrocenylmethyl group at the nitrogen, is obtained from the reaction of 1-aminomethylferrocene with 1,1′-bis(hydroxymethyl)ferrocene. Table 1 summarizes results of the reactions. Yields of **1** and **2** (19% and 30%) as well as that of *N*-hexyl-2-aza-[3]-(1,1′)-ferrocenophane (40%)[12] are lower than those of *N*-arylated azaferrocenophane from similar reactions reported previously (56–68%).[12] Although 6-aminohexanol causes not only condensation of the NH_2 group with 1,1′-bis(hydroxymethyl)ferrocene but also undesired self-condensation of the NH_2 and OH groups, the product **1** can be isolated in a pure form after purification by column chromatography

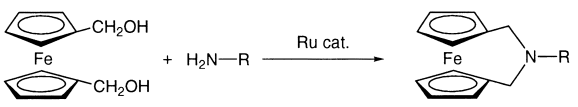

Scheme 1.

Table 1. Yields and Analytical Data of *N*-Substituted-2-aza-[3]-(1,1′)-ferrocenophanes

Product	Amine	Yield[a]	Color	Elemental Analysis[b]		
	R in RNH_2	%		C	H	N
1	$-(CH_2)_6$-OH	19	Yellow	65.80 (66.07)	6.42 (7.70)	4.33 (4.28)
2	-*cyclo*-C_6H_{11}	30	Yellow	70.26 (69.91)	7.30 (7.50)	4.34 (4.53)
3	$-(CH_2)_4Ph$	56	Yellow	72.99 (73.54)	7.08 (7.01)	3.82 (3.90)
4	$-C_6H_4$-*o*-^{i}Pr	32	Orange	73.28 (73.05)	7.00 (7.01)	3.85 (3.90)
5[c]	$-CH_2C_6H_4CF_3$	35	Orange	62.07 (62.36)	4.84 (4.71)	3.56 (3.64)
6	$-CH_2Fc$[d]	49	Orange	64.71 (64.98)	5.28 (5.45)	3.02 (3.29)

a) Isolated yield after purification by column chromatography and/or recrystallization.
b) Required values are given in parenthesis. c) F: 14.79 (14.50) d) Fc = ferrocenyl.

and recrystallization. 2-Isopropylaniline also undergoes the condensation with 1,1′-bis(hydroxymethyl)ferrocene to afford **4** in 32% yield, indicating that the presence of the bulky substituent at *ortho* position does not block the C–N bond formation. The OH group of **1** was substituted with iodine atom by the reaction of **1** with NaI in the presence of P_2O_5 and $Me_3SiOSiMe_3$ to give **7**, which has a 6-iodohexyl substituent at the nitrogen, as shown in Eq. 2.[13,14]

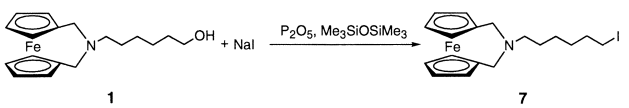

1 7

(2)

The ferrocenophanes **1**–**7** were characterized by means of NMR spectroscopy and elemental analyses. For example, the ^{1}H NMR spectrum of **1** contains an AB doublet at δ 4.08 and 4.07 due to the cyclopentadienyl hydrogens and a singlet of the $CpCH_2$ hydrogens at δ 2.89. The OH hydrogen signal is observed at δ 1.57. The ^{13}C{^{1}H} NMR spectrum exhibits the OCH_2, NCH_2(6-hydroxyhexyl), and NCH_2Cp carbon signals at δ 63.0, 57.6 and 52.2, respectively. The peak positions are close to the corresponding hydrogen signals of analogous *N*-alkyl-2-aza-[3]-(1,1′)-ferrocenophanes. Ferrocenophanes **2**–**5** also give reasonable NMR spectra for the proposed structure. The ^{1}H and ^{13}C{^{1}H} NMR spectra of **6** indicate the presence of 1,1′-disubstituted ferrocenylene and 1-substituted ferrocenyl groups. The two CH_2 hydrogen signals are observed at δ 3.84 and 2.85 in a 1:2 peak area ratio. These spectroscopic data as well as analytical results confirm the *N*-ferrocenomethyl-2-aza-[3]-(1,1′)-ferrocenophane structure.

N-Alkyl-2-aza-[3]-(1,1′)-ferrocenophanes **1**–**3** undergo two electrochemical oxidation reactions at different potentials, as described below. Figure 1a depicts the cyclic voltammogram of **1**, which shows two oxidation waves, at 0.06 V and 0.44 V (Ag^+/Ag). The former electrochemical reaction is reversible, since a scanning up to 0.20 V leads to reversible oxidation and reduction waves at $E_{pc} - E_{pa} = 98$ mV. Similar two step redox was obtained for **2** and **3**, as summarized in Table 2. Cyclic voltammograms of **4** and **5** show electrochemical response of ferrocene-ferrocenium redox only. The electrochemical measurement of **6** was not feasible, partly due to its low solubility in polar organic solvents.

Our previous study[12] revealed that the *N*-aryl-2-aza-[3]-(1,1′)-ferrocenophanes exhibit an irreversible electrochemical oxidation at E_{ox} = 0.68–0.75 V and that *N*-hexyl-2-aza-[3]-(1,1′)-ferrocenophane shows the corresponding oxidation wave at a lower potential ($E_{1/2}$ = 0.44 V). The reaction was assigned to the electrochemical oxidation of the NCH_2 group of the ligand accompanied by deprotonation as shown in Scheme 2 (i). The initially formed ferrocenium (**A**) is in equilibrium with (**A′**) having Fe(II) center and a cation radical at the nitrogen atom via rapid and reversible electron transfer between Fe and N atoms.[15] Further oxidation of the ligand accompanied by proton elimination leads to the product having an iminium structure (**B**). The latter reaction lacks in reversibility, due to low affinity of the iminium group and H^+ under the electrochemical reduction conditions. The fact that the oxidation potential of **1**–**3** with *N*-alkyl substituents is lower than that of the *N*-aryl derivatives can be attributed to the basicity of the alkyl amines being higher than that of the aryl amines. The electrochemical behavior of *N*-aryl-2-aza-[3]-(1,1′)-ferrocenophanes, *N*-(4-*t*-butylphenyl)-2-aza-[3]-(1,1′)-ferrocenophane and *N*-(4-hydroxyphenyl)-2-aza-[3]-(1,1′)-ferrocenophane (**8**),[12] is compared in Figs. 1b and c. Both compounds exhibit the redox between ferrocene and ferrocenium at similar positions ($E_{1/2}$ = 0.04 and −0.02 V, respectively). The former compound shows a second oxidation at E_{ox} = 0.75 V with low reversibility, whereas **8** undergoes reversible electrochemical oxidation and reduction at a lower potential ($E_{1/2}$ = +0.44 V). Scheme 2 (ii) depicts the mechanism which accounts for the unique electrochemical behavior of **8**. The initial oxidation of **8** produces a ferrocenium (**C**) which is in equilibrium with the ferrocenophane-containing cation radical at the nitrogen atom (**C′**) similarly to Scheme 2 (i). Further oxidation and deprotonation

Table 2. Results of Cyclic Voltammetry

Compound	Electrochemical Potential/V (vs Ag^+/Ag)[a]		
	$E_{1/2}$ ($I^- \leftrightarrow I_2$)[b]	$E_{1/2}$ (Fe(II) ↔ Fe(III))	E_{ox} (amine)[b]
1		−0.01 (0.10)	+0.44
2		−0.01 (0.15)	+0.42
3		+0.04 (0.09)	+0.41
4		+0.04 (0.12)	—[c]
5		+0.04 (0.06)	—[c]
9-I^-	−0.11	+0.42 (0.06)	
9-BF_4^-		+0.42 (0.07)	
12-I^-	−0.15	+0.37 (0.09)	
12-BF_4^-		+0.39 (0.10)	

a) ΔE (= $E_{pc} - E_{pa}$, V) is shown in parentheses.
b) Irreversible oxidation. c) Not observed clearly.

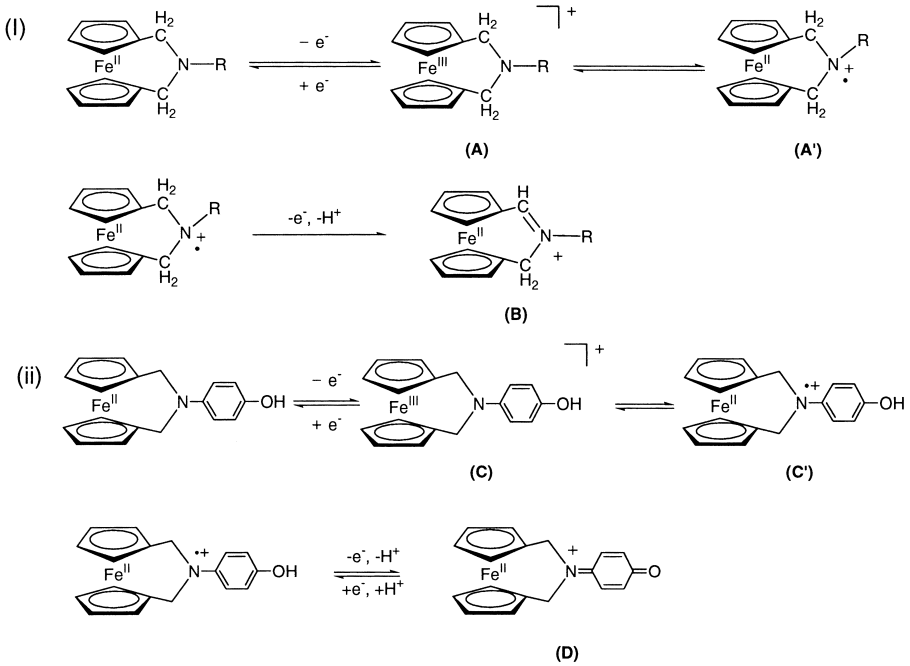

Scheme 2.

of the OH group affords the species with a iminium quinone structure in the ligand (**D**). The stability of (**D**) is much higher than that of (**B**); this is probably the primary reason for the oxidation potential of **8** being lower than those of **7** and the other *N*-aryl-2-aza-[e]-ferrocenophanes. Since protonation of the oxygen of **D** takes place to regenerate the ferrocenium (**C**) easily under the electrochemical reduction conditions, the total electrochemical process shown in Scheme 2 (ii) occurs with high reversibility.

Figure 2 depicts absorption spectra obtained during the electrochemical oxidation of **8** using a flow electrolysis cell.[16] Before oxidation, the spectrum (a) contains an absorption due to **8** (247 nm) exclusively. Oxidation up to 0.0 V leads to a decrease in the peak at UV region and to concomitant growth of new peaks at 375 and 535 nm. They can be assigned to the nitrogen radical cation of (**C′**) in Scheme 2 (ii) and ferrocenium cation (**C**), respectively, based on comparison of the spectrum with those of oxidized polyaniline and ferrocenium.[17] At higher potentials (above 0.30 V), a new absorption band at nearly 800 nm is observed, which is ascribed to further oxidation of the *N*-substituent and deprotonation of the OH group, affording the species with a quinone-imine structure (**D**). The reaction pathway shown in Scheme 2 is consistent with the above electrochemical and spectroscopic measurements, although the intermediates in the Scheme were not fully identified.

As reported previously, *N*-hexyl-2-aza-[3]-(1,1′)-ferrocenophane reacts with MeI to produce the quaternary ammonium derivative **9-I**$^-$ (Eq. 3).[12] The reaction of *N*-alkyl-2-aza-[3]-(1,1′)-ferrocenophanes (**1**–**3**) with MeI also give the corresponding *N*-methylated cationic compounds, **10-I**$^-$, **11-I**$^-$, and **12-I**$^-$, respectively, as shown in Eq. 3. The iodo counter anion is easily replaced with BF_4^- by addition of $AgBF_4$ to a solution of the quaternary group containing ferrocenophanes (Eq. 4). PF_6^- salt of the cationic *N*-methylated ferrocenophane **12-PF$_6$**$^-$ was obtained from a one-pot reaction of **3** with MeI and subsequent addition of NH_4PF_6 to the reaction mixture (Eq. 5).

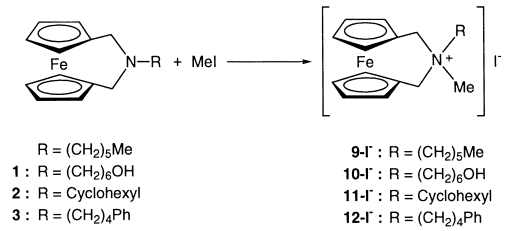

(3)

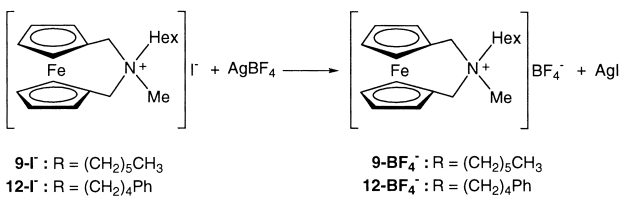

(4)

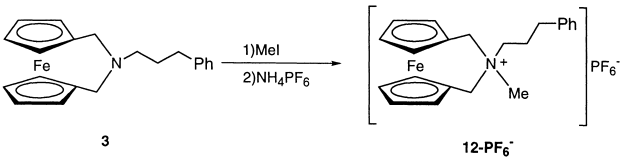

(5)

The structures of these complexes were confirmed by NMR spectroscopy and X-ray crystallography. Figure 3 displays structures of the cationic part of **10-I**$^-$, **11-I**$^-$, and **12-PF$_6$**$^-$. These cationic ferrocenophanes have the quaternary nitrogens with an almost tetrahedral structure. The N–C bonds in average are longer than those of neutral azaferrocenophanes due to the presence of positive charge, as summarized in Table 3. Separation of the iodo anion from the cationic part of the ferrocenophanes is sufficiently large in the solid state. Figure 4

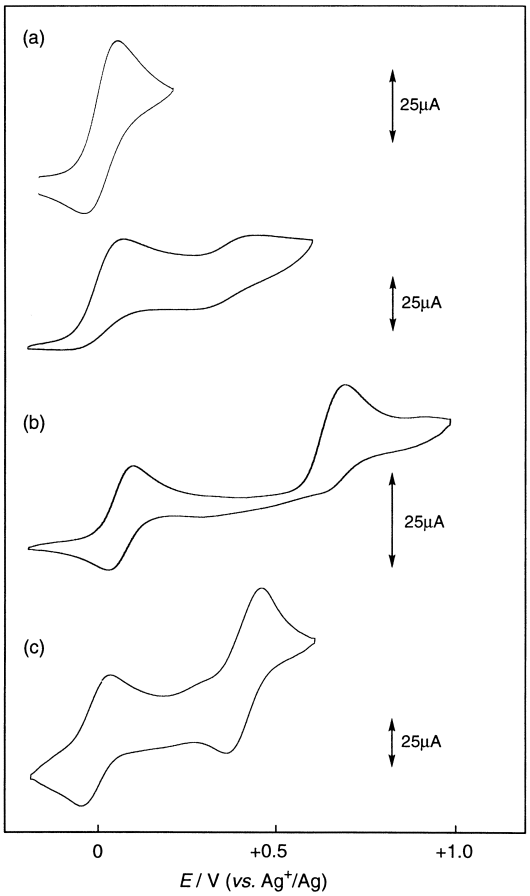

Fig. 1. Cyclic voltammograms of (a) **1**, (b) *N*-(4-*t*-butylphenyl)-2-aza-[3]-(1,1′)-ferrocenophane (c) *N*-(4-hydroxyphenyl)-2-aza-[3]-(1,1′)-ferrocenophane in MeCN solutions containing Et_4NBF_4 (0.10 M) (scan rate = 100 mV s^{-1}). The $E_{1/2}$ values of (b) ($E_{1/2}$ = +0.04 and +0.45 V) and (c) ($E_{1/2}$ = +0.04 and +0.44 V) shown in our previous report[12] were not correct, but are actually (b) $E_{1/2}$ = +0.06 (ΔE = 0.07 V) and +0.67 V (ΔE = 0.06 V) and (c) $E_{1/2}$ = −0.02 (ΔE = 0.07 V) and +0.41V (ΔE = 0.08 V). These results were not discussed in detail in our previous paper.

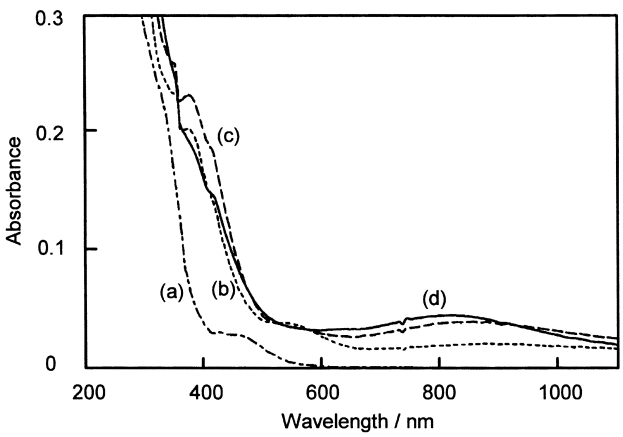

Fig. 2. Absorption spectra of 1.0×10^{-4} M of *N*-(4-hydroxyphenyl)-2-aza-[3]-ferrocenophane (**8**) in MeCN solutions containing Et_4NBF_4 (0.10 M) at (a) −0.40 V, (b) +0.00 V, (c) +0.30 V, and (d) +0.40 V (vs Ag^+/Ag).

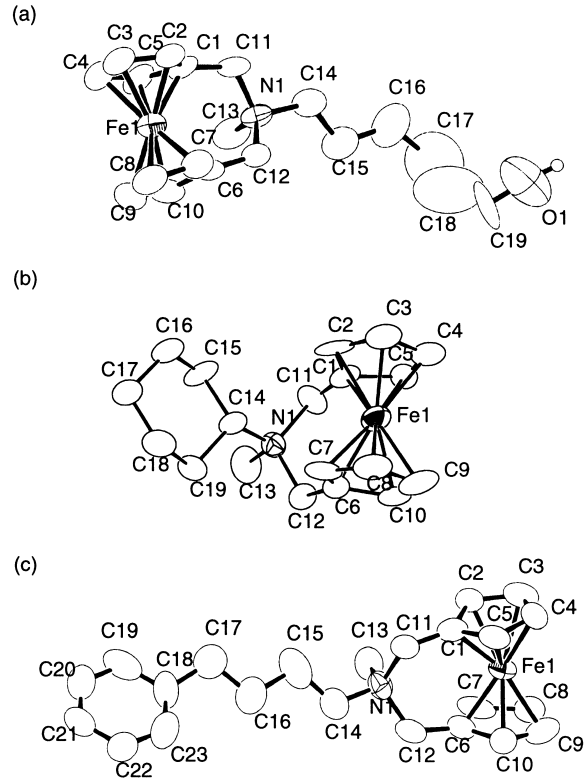

Fig. 3. Molecular structures of **10-I**$^-$, **11-I**$^-$, and **12-PF$_6$**$^-$ determined by X-ray crystallography. Counter anions and hydrogen atoms are omitted for simplicity. As for **10-I**$^-$, one of the two crystallographically independent molecules is shown.

Table 3. Selected Bond Distances and Angles

	10-I$^-$[a)]		**11-I**$^-$	**12-PF$_6$**$^-$
N1–C11	1.519(9)	1.546(9)	1.57(1)	1.53(1)
N1–C12	1.55(1)	1.516(9)	1.54(1)	1.56(1)
N1–C13	1.50(1)	1.49(1)	1.50(1)	1.52(1)
N1–C14	1.53(1)	1.52(1)	1.55(1)	1.52(1)
N1–C11–C1	118.2(8)	118.6(7)	116.5(9)	119.3(8)
N1–C12–C6	119.3(8)	118.7(7)	118(1)	119.4(8)

a) The parameters in the right column of **10-I**$^-$ are those of the crystallographically independent molecule.

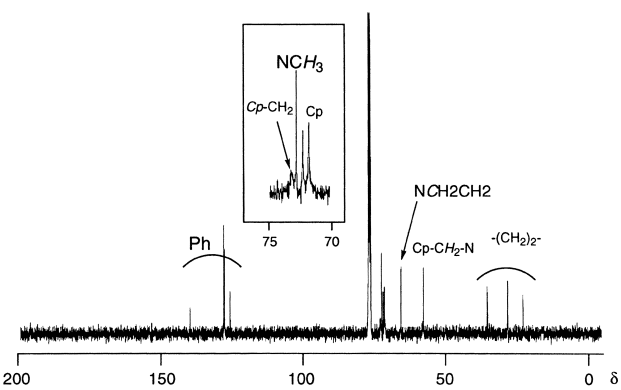

Fig. 4. $^{13}C\{^1H\}$ NMR spectrum of **12-I**$^-$ in $CDCl_3$.

shows the $^{13}C\{^1H\}$ NMR spectrum of **12-I**$^-$ in $CDCl_3$. Peaks of the NCH_2 carbon (δ 65.8) and Cp-CH_2 carbon (δ 57.9) appear at significantly lower positions than the corresponding carbon peaks of non-methylated ferrocenophane **3** (δ 57.4 and 52.3, respectively) owing to the existence of the positive charge at the nitrogen. The ^1H NMR spectra of **12-I**$^-$ and **12-BF$_4$**$^-$ are similar but not exactly identical to each other, which may suggest the presence of weak interaction between the cationic ferrocenophane and the counter ion in solution. Storage of the solution of **12-I**$^-$ for several days caused color change of the solution to red brown, probably due to formation of I_2 in solution, although the ferrocene-containing product was not characterized. **12-BF$_4$**$^-$ shows much higher stability than **12-I**$^-$ in solution.

Figure 5 depicts cyclic voltammograms of **12-I**$^-$ and **12-BF$_4$**$^-$ in addition to the non-*N*-methylated neutral ferrocenophane **3**. **12-I**$^-$ exhibits the irreversible oxidation of I^- to I_2 at $E_{1/2} = -0.15$ V (vs Ag^+/Ag, $E_{ox} = -0.04$ V) and two additional reversible redoxes leading to two pairs of oxidation and reduction peaks. The large peaks at $E_{1/2} = +0.37$ V are in positions close to those of **12-BF$_4$**$^-$ (0.39 V), indicating that the electrochemical reaction corresponds to oxidation and reduction of the Fe center of cationic ferrocenophane **12-I**$^-$. Why the oxidation potentials of **12-I**$^-$ and **12-BF$_4$**$^-$ are higher than the potentials of **3** ($E_{1/2} = +0.03$ V) can be rationalized by the existence of positive charge at the nitrogen atom close to the Fe center, which prevents facile electrochemical oxidation around the nitrogen atom. Such smaller electrochemical peaks of **12-I**$^-$ at +0.30 V may be assigned to a minor ferrocene-containing product due to the oxidation of the iodo counter ion because the cyclic voltammogram of **12-BF$_4$**$^-$ does not show such redox waves.

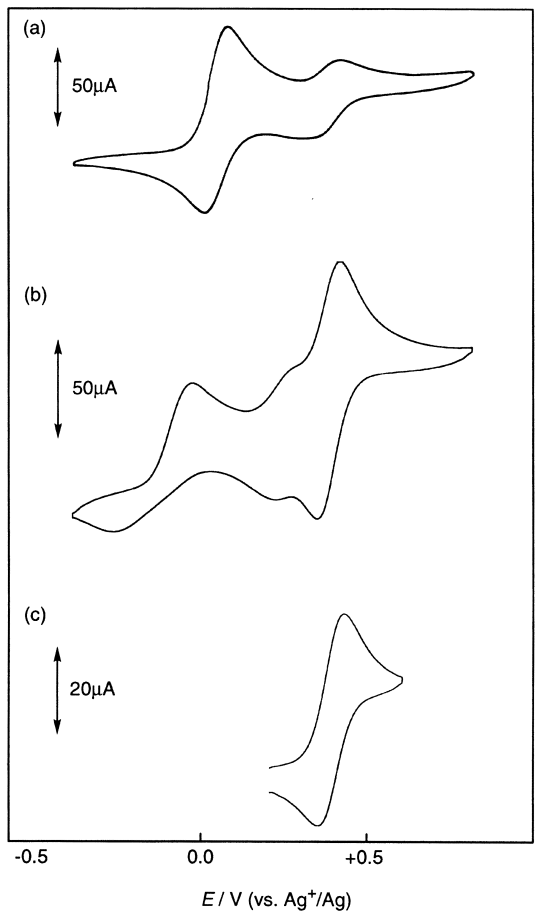

Fig. 5. Cyclic voltammograms of (a) **3**, (b) **12-I**$^-$, and (c) **12-BF$_4$**$^-$ in MeCN solutions containing Et_4NBF_4 (0.10 M) (scan rate = 100 mV s^{-1}).

N-alkyl- and *N*-aryl-2-aza-[3]-(1,1′)-ferrocenophanes prepared in our previous and present studies exhibit several kinds of unique chemical and electrochemical behavior. Since we also succeeded in immobilization of the ferrocenophanes in polymer matrices,[18] application of these for electrodes or catalysis can be expected.

Experimental Section

General Consideration, Materials, and Measurement. All the manipulations of $[RuCl_2(PPh_3)_3]$ were carried out under nitrogen or argon using standard Schlenk techniques. The NMR spectra (^1H and $^{13}C\{^1H\}$) were recorded on a JEOL EX-400 spectrometer at 25 °C unless otherwise stated. Elemental analyses were carried out by a Yanaco MT-5 CHN autocorder. Cyclic voltammetry was measured in MeCN solution containing 0.10 M Et_4NBF_4 with ALS Electrochemical Analyzer Model-600A. The Ag^+/Ag reference was used as the reference. Spectroelectrochemical measurements were carried out by using a combination of a flow through electrolysis cell, ALS Electrochemical Analyzer Model-600A and EYELA peristaltic pump SMP-11, and Shimadzu UV1600 spectrometer. Details of apparatus were reported previously.[16] $[RuCl_2(PPh_3)_3]$ and 1,1′-bis(hydroxymethyl)ferrocene were prepared according to literature methods.[19,20] Acetonitrile and 1-methyl-2-pyrrolidinone (NMP) were dried over CaH_2, distilled, and stored under nitrogen or argon. Et_4NBF_4 for the electrochemical measurement was recrystallized from methanol before use.

Preparation of 1–6. To an NMP (3 cm^3) solution of $[RuCl_2(PPh_3)_3]$ (67 mg, 0.070 mmol) was added 6-aminohexanol (234 mg, 2.0 mmol) and then 1,1′-bis(hydroxymethyl)ferrocene (492 mg, 2.0 mmol) at room temperature. The mixture was heated at 180 °C for 24 h. After the solution was evaporated under vacuum, the remaining residue was dissolved in ethyl acetate to remove the insoluble fraction by filtration. The soluble material was purified by column chromatography (silica gel, hexane:ethyl acetate = 2:1) and was recrystallized from a chloroform–methanol mixture to afford **1** as a yellow solid (124 mg, 19%). ^1H NMR ($CDCl_3$) δ 4.08, 4.07 (d, 8H, Cp, J = 2 Hz), 3.68 (t, 2H, CH_2OH), 2.89 (s, 4H, Cp-CH_2-N), 2.69 (t, 2H, NCH_2, J = 7 Hz), 1.62 (m, 4H, NCH_2 and CH_2OH), 1.57 (s, 1H, OH), 1.44 (q, 4H, (CH_2)$_2$CH$_2$OH). $^{13}C\{^1H\}$ NMR (100 MHz, in $CDCl_3$ at 25 °C) δ 83.2 (Cp-CH_2-N), 69.8, 69.1 (Cp), 63.0 (CH_2OH), 57.6 (NCH_2), 52.2 (Cp-CH_2-N), 32.8, 27.6, 27.2, 25.6 (CH_2).

Other *N*-substituted-2-aza-[3]-(1,1′)-ferrocenophanes **2**–**6** were prepared analogously and their data are shown below. NMR data of **2**. Abbreviation of hydrogens is shown in Chart 1. ^1H NMR

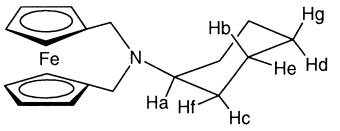

Chart 1.

($CDCl_3$) δ 4.08, 4.04 (d, 8H, Cp, J = 2 Hz), 3.02 (s, 4H, Cp-CH_2-N), 2.72 (tt, 1H, NCH_a, J = 3, 12 Hz), 1.90 (d, 2H, H_b, J = 12 Hz), 1.83 (d, 2H, H_c, J = 12 Hz), 1.65 (m, 1H, H_d), 1.36 (m, 2H, H_e), 1.27 (m, 2H, H_f), 1.14 (tt, 1H, H_g, J = 3, 12 Hz). $^{13}C\{^1H\}$ NMR (100 MHz, in $CDCl_3$ at 25 °C) δ 84.4 (*Cp*-CH_2-N), 69.8, 68.8 (Cp), 64.9 (N*C*H), 48.8 (Cp-*C*H_2-N), 29.7 (NCH*C*H_2) 26.5, 26.4 (NCHCH_2*C*H_2*C*H_2).

NMR data of **3**. ^1H NMR ($CDCl_3$) δ 7.30 (t, 2H, *meta*, J = 7 Hz), 7.21 (d, 2H, *ortho*, J = 7 Hz), 7.19 (t, 1H, *para*, J = 7 Hz), 4.08, 4.07 (d, 8H, Cp, J = 2 Hz), 2.88 (s, 4H, Cp-CH_2N), 2.71 (t, 2H, NC*H*, J = 8 Hz), 2.69 (t, 2H, PhCH_2, J = 8 Hz), 1.74 (quintet, 2H, NCH$_2$CH_2, J = 7 Hz), 1.67 (quintet, 2H, PhCH$_2$CH_2, J = 8 Hz). $^{13}C\{^1H\}$ NMR (100 MHz, in $CDCl_3$ at 25 °C) δ 142.7 (*ipso*, C_6H_5), 128.4, 128.3, 125.7 (*ortho*, *meta*, *para*, C_6H_5), 83.8 (*Cp*-CH_2-N), 69.8, 69.0 (Cp), 57.4 (NCH_2CH_2), 52.3 (CpCH_2-N), 35.8 (PhCH_2), 29.3 (NCH$_2$*C*H$_2$), 27.3 (PhCH*C*H$_2$).

NMR data of **4**. ^1H NMR ($CDCl_3$) δ 7.15–7.35 (m, 4H, Ph), 4.24, 4.15 (d, 8H, Cp, J = 3 Hz), 3.81 (m, CH_3CH-), 3.34 (s, 4H, Cp-CH_2-), 1,28 (d, 6H, CH_3). $^{13}C\{^1H\}$ NMR (100 MHz, in $CDCl_3$ at 25 °C) δ 145.0 (*ipso*, NC_6H_5), 126.3, 126.3, 125.1, 122.4 (*ortho*, *meta*, *para*, NC_6H_5), 83.5 (*Cp*-CH_2-N), 70.0, 69.5 (Cp), 53.5 (CpCH_2-N), 26.6 (CH_3*C*H), 23.6 (*C*H$_3$CH).

NMR data of **5**. ^1H NMR ($CDCl_3$) δ 7.61, 7.56 (d, 4H, Ph, J = 9 Hz), 4.12, 4.09 (d, 8H, Cp, J = 2 Hz), 3.89 (s, 2H, CH_2-N), 2.90 (s, 4H, Cp-CH_2-N). $^{13}C\{^1H\}$ NMR (100 MHz, in $CDCl_3$ at 25 °C) δ 144.1 (*para*, $C_6H_4CF_3$), 129.2 (*ipso*, $C_6H_4CF_3$, $^2J_{(C-F)}$ = 29 Hz), 129.0 (*meta*, $C_6H_4CF_3$), 125.2 (*ortho*, $C_6H_4CH_3$, $^3J_{(C-F)}$ = 4 Hz), 124.3 (*C*F$_3$, $^1J_{(C-F)}$ = 271 Hz), 83.1 (*Cp*-CH_2-), 69.8, 69.2 (Cp), 61.3 (C_6H_4-*C*H_2-N), 52.3 (Cp-*C*H_2-N).

NMR data of **6**. ^1H NMR ($CDCl_3$) δ 4.22 (t, 2H, H_a, J = 3 Hz), 4.15 (m, 6H, H_b and H_f), 4.05 (m, 9H, H_c and H_g), 3.84 (s, 2H, H_d), 2.85 (s, 4H, H_c) (Chart 2). $^{13}C\{^1H\}$ NMR (100 MHz, in $CDCl_3$ at 25 °C) δ 83.2 (*Cp*-CH_2-N), 83.2 (*Cp*-CH_2-N), 70.2, 69.5, 69.1, 68.5, 67.9 (Cp), 57.9 (Cp-*C*H_2-N), 51.1 (crosslinked Cp-*C*H_2-N).

***N*-(6-Iodohexyl)-2-aza-[3]-(1,1′)-ferrocenophanes (7).** Preparation was carried out according to the reported procedure with slight modification as follows.[13,14] A mixture of phosphorus pentoxide (1.31 g, 9.2 mmol), hexamethyldisiloxane (1.49g, 9.2 mmol), and dry benzene (15 cm^3) was refluxed for 30 min until the mixture became a clear solution. The solvent was removed and toluene (5 cm^3), sodium iodide (138 mg, 0.92 mmol), **1** (260 mg, 0.80 mmol) were added in this order at room temperature. The reaction mixture was heated at 50 °C for 24 h with stirring. A saturated aqueous sodium bicarbonate solution containing sodium thiosulfate was added to quench the reaction. The organic products were extracted with ether repeatedly. The combined extracts were washed with brine and the solvent was evaporated. The crude product was purified by column chromatography (silica gel, $CHCl_3$:MeOH = 95.5) to **6** as a yellow solid (215 mg, 61%). Anal. Calcd for $C_{18}H_{24}FeNI$: C, 49.46; H, 5.53; N, 3.20; I, 29.03%. Found: C, 48.68; H, 5.39; N, 2.97; I, 28.98%. ^1H NMR ($CDCl_3$) δ 4.16, 4.09 (d, 8H, Cp, J = 2 Hz), 3.22 (t, 2H, CH_2I, J = 7 Hz), 3.00 (s, 4H, Cp-CH_2-N), 2.77 (t, 2H, NCH_2, J = 7 Hz), 1.87 (quintet, 2H, ICH$_2$CH_2), 1.67 (quintet, 2H, NCH$_2$CH_2), 1.46 (m, 4H, CH_2). $^{13}C\{^1H\}$ NMR (100 MHz in $CDCl_3$ at 25 °C) δ 82.5 (*Cp*-CH_2-N), 70.0, 69.4 (Cp), 57.6 (NCH_2), 52.1 (Cp-*C*H_2-N), 33.5, 30.3, 27.0, 26.3 (CH_2(*C*H$_2$)$_4$*C*H$_2$), 7.01 (*C*H$_2$I).

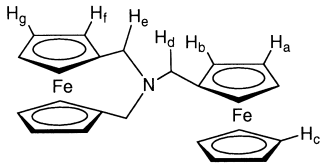

Chart 2.

Preparation of 10-I$^-$–12-I$^-$. To the MeCN (5 cm^3) suspension of **1** (63 mg , 0.19 mmol) was added MeI (81 mg, 0.57 mmol) at room temperature. Compound **1** was instantly dissolved on stirring. After 24 h, a crystalline product was separated from the solution and was collected by filtration. The resulting orange solid was recrystallized from $CHCl_3$/Et_2O (65 mg, 72%) to give **10-I$^-$**. Anal. Calcd for $C_{19}H_{28}FeINO$: C, 48.64; H, 6.02; N, 2.99; I, 27.05%. Found: C, 48.68; H, 5.95; N, 2.58; I, 26.50%. ^1H NMR ($CDCl_3$) δ 4.56, 4.50, and 4.47 (m, 4H, Cp*C*H$_2$N), 4.34 and 4.29 (8H, Cp ring), 3.88 (br, 2H, NCH_2CH$_2$), 3.68 (t, 2H, CH_2OH), 3.56 (s, 3H, Me), 1.96 (br, 2H, NCH$_2$CH_2), 1.61 (quintet, 2H, CH_2CH$_2$OH), 1.60 (s, 1H, OH), 1.56 (br, 4H, CH$_2$(CH_2)$_2$CH$_2$OH).

11-I$^-$ and **12-I$^-$** were obtained analogously from **2** and **3**, respectively. Analytical data of **11-I$^-$**. Anal. Calcd for $C_{23}H_{28}FeIN$: C, 50.58; H, 5.81; N, 3.10%. Found: C, 50.28; H, 5.79; N, 2.66%. NMR data of **12-I$^-$**. ^1H NMR ($CDCl_3$) δ 7.33–7.19 (Ph), 4.50, 4.53, 4.49 (m, 4H, Cp-CH_2N), 4.30–4.10 (br, 8H, Cp), 3.81 (m, 2H, NCH_2), 3.52 (s, 3H, Me), 2.76 (t, 2H, PhCH_2), 2.00–1.75 (m, 4H, NCH$_2$CH_2 and PhCH$_2$CH_2). $^{13}C\{^1H\}$ NMR (100 MHz, in $CDCl_3$ at 25 °C) δ 140.6 (*ipso*, C_6H_5), 128.7, 128.6, 126.3 (*ortho*, *meta*, *para*, C_6H_5), 73.1 (*Cp*-CH_2-N), 72.8 (Me), 72.3, 71.8 (Cp), 65.8 (NCH_2CH_2), 57.9 (Cp*C*H$_2$-N), 35.0, 27.9, 22.5 (CH_2).

NMR data of **11-I$^-$** and analytical data of **12-I$^-$** were not obtained.

Anion Exchange of 9-I$^-$ and 12-I$^-$ with $AgBF_4$. To an acetone (5 cm^3) suspension of **12-I$^-$** (95 mg, 0.19 mmol) was added $AgBF_4$ (37 mg, 0.19 mmol) at room temperature, then readily a white solid was precipitated. The reaction mixture was filtered to remove the AgI and evaporated at reduced pressure. The obtained crude products were recrystallized from $CHCl_3$/ether to lead **12-BF_4^-** as yellow crystals (67 mg, 76%). ^1H NMR ($CDCl_3$) δ 7.32–7.19 (Ph), 4.30, 3.90 (br, 8H, Cp), 4.39, 4.08 (s, 4H, Cp-CH_2N), 3.60 (m, 2H, NCH_2), 3.32 (s, 3H, Me), 2.75 (t, 2H, PhCH_2), 2.00–1.75 (m, 4H, NCH$_2$CH_2 and PhCH$_2$CH_2).

Anion exchange of **9-I$^-$** was carried out analogously.

Preparation of 12-PF_6^-. MeCN (5 cm^3) suspension of **3** (63 mg, 0.18 mmol) was added MeI (77 mg, 0.54 mmol) at room temperature. Compound **3** was instantly dissolved on stirring. After 24 h, a crystalline product was separated from the solution and was collected by filtration. The obtained crystals were dissolved in MeCN and NH_4PF_6 (32 mg, 0.20 mmol) was added. The reaction mixture was stirred for 1 h, then H_2O was added to precipitate the product. Solids were filtered and washed with H_2O repeatedly. The obtained crude products were recrystallized from $CHCl_3$/ether to give **12-PF_6^-** as orange crystals (76 mg, 82%). Anal. Calcd for $C_{23}H_{24}F_6FeNP$: C, 53.20; H, 5.43; N, 2.70%. Found: C, 53.53; H, 5.71; N, 2.62%.

Crystal Structure Determination. Crystals of **10-I$^-$**, **11-I$^-$**, and **12-PF_6^-** suitable for X-ray diffraction study were obtained by recrystallization from $CHCl_3$-Et_2O and mounted in glass capillary tubes under argon. Intensities were collected for Lorentz and polarization effects on a Rigaku AFC-5R automated four-cycle diffractometer by using Mo-$K\alpha$ radiation (λ = 0.71069 Å) and ω-2θ scan method, and an empirical absorption correction (Ψ scan) was applied. Calculations were carried out using a program package TEXSAN for Windows. Atomic scattering factors were obtained from the literature.[21] A full matrix least-squares refinement was

Table 4. Crystallographic Data of **10-I**$^-$, **11-I**$^-$, and **12-PF$_6$**$^-$

	10-I$^-$	**11-I**$^-$	**12-PF$_6$**$^-$
Formula	$C_{19}H_{28}FeNOI$	$C_{19}H_{26}FeNI$	$C_{23}H_{28}FeNPF_6$
M	469.19	451.17	519.29
Crystal Size	$0.5 \times 0.6 \times 0.8$	$0.4 \times 0.4 \times 0.6$	$0.5 \times 0.9 \times 1.0$
Crystal system	monoclinic	monoclinic	monoclinic
Space group	$P2_1/c$ (No. 14)	$P2_1/c$ (No. 14)	Cc (No. 9)
a/Å	12.507(5)	7.169(3)	10.534(5)
b/Å	20.669(7)	17.504(3)	16.805(5)
c/Å	15.001(7)	14.965(4)	13.466(6)
β/deg	93.30(2)	96.04(3)	107.40(3)
V/Å^3	3871(2)	1867.3(8)	2275(2)
Z	4	4	4
μ(Mo$K\alpha$)/ mm^{-1}	2.378	2.458	0.792
Unique reflections	7694	4445	2694
Used reflections ($I > 3.00\sigma(I)$)	3197	2182	1890
R (F_0)	0.047	0.068	0.066
R_w (F_0)	0.043	0.048	0.056

used for non-hydrogen atoms with anisotropic thermal parameters. Hydrogen atoms were located by assuming the ideal geometry and these locations were included in the structure calculation without further refinement of the parameters. Crystallographic data and details of refinement are summarized in Table 4. All the data of the crystallographic study including F_o-F_c tables are deposited as Document No. 74059 at the Office of the Editor of Bull. Chem. Soc. Jpn. Crystallographic data are deposited also at the CCDC, 12 Union Road, Cambridge CB2 1EZ, UK and copies can be obtained on request, free of charge, by quoting the publication citation and the deposition numbers 169227–169229.

This work was financially supported by a Grant-in-Aid for Scientific Research from the Ministry of Education, Culture, Sports, Science and Technology.

References

1 "Ferrocenes," ed by A. Togni and T. Hayashi, VCH, New York (1995).

2 W. R. Cullen and J. D. Woolins, *Coord. Chem. Rev.*, **39**, 1 (1981).

3 T. Hayashi and M. Kumada, *Acc. Chem. Res.*, **15**, 195 (1982).

4 J. S. Miller and A. J. Epstein, *Angew. Chem., Int. Ed. Engl.*, **33**, 385 (1994).

5 S. Barlow and S. R. Marden, *Chem. Commun.*, **2000**, 1555.

6 H. Nishihara, *Bull. Chem. Soc. Jpn.*, **74**, 19 (2001).

7 S.-I. Murahashi, K. Kondo, and T. Hakata, *Tetrahedron Lett.*, **23**, 229 (1982).

8 Y. Watanabe, Y. Tsuji, H. Ige, Y. Ohsugi, and T. Ohta, *J. Org. Chem.*, **49**, 3359 (1984).

9 Y. Tsuji, K.-T. Huh, Y. Ohsugi, and Y. Watanabe, *J. Org. Chem.*, **50**, 1365 (1985).

10 Y. Tsuji, K.-T. Huh, Y. Yokoyama, and Y. Watanabe, *J. Chem. Soc., Chem. Commun.*, **1986**, 1575.

11 Y. Tsuji, Y. Yokoyama, K.-T. Huh, and Y. Watanabe, *Bull. Chem. Soc. Jpn.*, **60**, 3456 (1987).

12 T. Sakano, H. Ishii, I. Yamaguchi, K. Osakada, and T. Yamamoto, *Inorg. Chim. Acta*, **296**, 176 (1999).

13 T. Iwamoto, T. Matsumoto, T. Kusumoto, and M. Yokoyama, *Synthesis*, **1983**, 460.

14 T. Iwamoto, H. Yokoyama, and M. Yokoyama, *Tetrahedron Lett.*, **22**, 1803 (1981).

15 H. Plenio, J. Yang, R. Diodone, and J. Heinze, *Inorg. Chem.*, **33**, 4098 (1994).

16 H. Nakao, H. Hayashi, and K. Okita, *Anal. Sci.*, **17**, 545 (2001).

17 B. Divisia-Blohorn and M. Paltrier, *Inorg. Chim. Acta*, **131**, 65 (1987).

18 T. Sakano and K. Osakada, *Macrmomol. Chem. Phys.*, **202**, 1829 (2001).

19 P. S. Hallman, T. A. Stephenson, and G. Wilkinson, *Inorg. Synth.*, **12**, 237 (1970).

20 A.-S. Carlström and T. Frejd, *J. Org. Chem.*, **55**, 4175 (1990).

21 "International Tables for X-Ray Crystallography," Kynoch; Birmingham, England (1974), Vol. 4.